First-principle and data-driven model-based approach in rotating machinery failure mode detection

G. Wszołek [a], P. Czop [b],*

[a] Institute of Engineering Processes Automation and Integrated Manufacturing Systems,
Silesian University of Technology, ul. Konarskiego 18a, 44-100 Gliwice, Poland
[b] Tenneco Automotive Eastern Europe, Eastern European Engineering Center (EEEC),
ul. Bojkowska 59 B, 44-100 Gliwice, Poland
* Corresponding author: E-mail address: piotr.czop@labmod.com

Analysis and modelling

ABSTRACT

Purpose: A major concern of modern diagnostics is the use of vibration or acoustic signals generated by a machine to reveal its operating conditions. This paper presents a method which allows to periodically obtain estimates of model eigenvalues represented by complex numbers. The method is intended to diagnose rotating machinery under transient conditions.

Design/methodology/approach: The method uses a parametric data-driven model, the parameters of which are estimated using operational data.

Findings: Experimental results were obtained with the use of a laboratory single-disc rotor system equipped with both sliding and hydrodynamic bearings. The test rig used allows measurements of data under normal, or reference, and malfunctioning operation, including oil instabilities, rub, looseness and unbalance, to be collected.

Research limitations/implications: Numerical and experimental studies performed in order to validate the method are presented in the paper. Moreover, literature and industrial case studies are analyzed to better understand vibration modes of the rotor under abnormal operating conditions.

Practical implications: A model of the test rig has been developed to verify the method proposed herein and to understand the results of the experiments. Hardware realization of the proposed method was implemented as a standalone operating module developed using the Texas Instruments TMS3200LF2407 Starter Kit.

Originality/value: The parametric approach was proposed instead of nonparametric one towards diagnosing of rotating machinery.

Keywords: First-principle model; Data-driven model; Grey-box; Servo-hydraulic system

1. Introduction

A major concern of modern diagnostics is the use of vibration or acoustic signals generated by a machine to reveal its operating conditions [1-4]. The produced vibrations are used to detect malfunctions or changes in the vibration paths. The intensive development of diagnostic routines aimed at vibration assessment was initiated in the 1980s. This was a result of the continuing development of data acquisition systems and awareness of the importance of diagnostics [5]. The majority of the implemented improvements have gradually been introduced into practice. The fundamentals of signal-processing and the interpretation of machinery performance characteristics were also deduced from theoretical studies [6]. In the 1990s, existing approaches to data interpretation and their processing were already being continually improved [7], and computer networks were being implemented, facilitating readily available information acquisition and enabling access from almost any location, both at the plant and remotely [8]. Owing to the potential for higher performance and prolonged service time, special attention is usually paid to modern early-warning diagnostic systems. Because Alignment, Balance, and incorrect Clearances (ABC) are the most common problems affecting rotating machinery in terms of severity [9], efforts should therefore focus on Early Warning (EW) diagnostics and on increasing ABC malfunction detectability (Fig. 1).
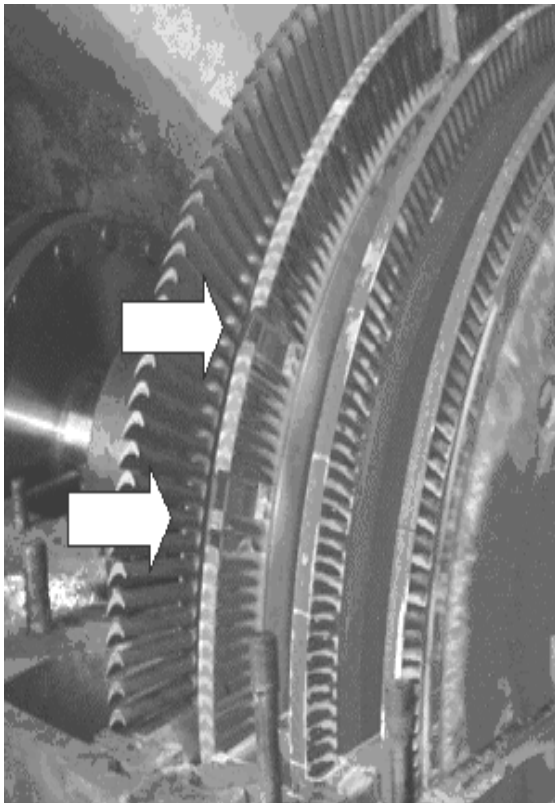

Fig. 1. A servo-hydraulic test-rig used in experimental investigations

Besides complex diagnostic solutions dedicated to large machinery, simple and less expensive ones have been launched into the market. Up to now, small and medium-size machinery (e.g. mills, fans, compressors and pumps) with auxiliary devices have rarely been monitored because of the relatively high costs of diagnostic systems, compared to the costs of the machine and preventive maintenance. Available fault detection and isolation solutions are mainly based on non-parametric techniques using time-frequency domain analyses. In these solutions, the amplitude, frequency, and phase contents of the vibration signal are used to detect malfunctioning operation. Service specialists or experienced maintenance staff are responsible for selecting the relevant diagnostic symptoms and setting appropriate warning/alarm thresholds, e.g. amplitude-phase acceptance regions [10]. Nevertheless, this type of diagnostic knowledge and expertise is expensive and available only within a limited scope and time. For instance, the temporary absence of a maintenance staff member may cause a temporary drop in the quality of diagnostic expertise. Moreover, the expertise provided by specialists can differ even when we consider similar plants equipped with similar machinery. Therefore, automatic and self-inference solutions are valuable and still required to eliminate the need for expert service, even if they are more expensive.

Therefore, the proposed approach towards the detection of ABC malfunctions considers recent trends in parametric system identification, providing possibilities for semi-automatic diagnostic scenarios using physical interpretation of the obtained results. The most important advantage is that a parametric model approach can yield higher resolutions than non-parametric ones in cases where the signal length is relatively short. This is the case for transient startup and coastdown conditions lasting from a few seconds for small-size machinery to a couple of minutes for medium-size machinery. On the other hand, better sensitivity and selectivity of parametric methods enables earlier detection of pending failures, e.g. rotor cracks. Nevertheless, diagnostic expertise is still required to choose adequate symptoms of failure modes.

2. The method

The paper presents an application of AR (AutoRegressive) time series models for the detection of changes in the eigenfrequencies and dampings of the rotating machinery. The AR model is also known as an all-pole linear filter with all of its zeros at the origin in the z-plane from a signal processing theory point of view. The AR models were successfully used to estimate the power spectrum of periodic signals characterized by harmonic components [11]. The AR model has the form of a discrete transfer function, where the denominator parameters are identified with the least-square algorithm. There are a few estimator algorithms of AR model parameters, such as Yule-Walker, Burg, covariance, and the modified covariance method, that have different properties summarized in [12]. A parametric approach involving AR models used at the stage of fault detection provides a few important advantages compared to a non-parametric approach, such as: high resolution in the frequency domain, the possibility of non-stationary process modeling, and estimation of non-biased parameters for data heavily corrupted by noise. The

AR model can also be represented in the form of a non-parametric model, e.g. power spectrum, autocorrelation function, and impulse/step time domain response.

The parameters of the estimated AR model are uncertain, due to disturbances in the observed data and other inaccuracies, e.g. the 'true' model structure [12]. An increase in a confidence interval can be interpreted as a decrease in model accuracy (Fig. 2). In the case of eigenvalues, i.e. poles, the confidence area is expressed as an ellipsoid, i.e. poles with two coordinates, imaginary and real, respectively [12]. In the case of a rigid rotor, where the ratio of a rotor diameter to its length is significant, the second or fourth order model is recommended. If a priori information is unavailable, then a model structure can be evaluated and properly selected from the measured data. Two of the most commonly applied tests are the AIC and MDL [12].
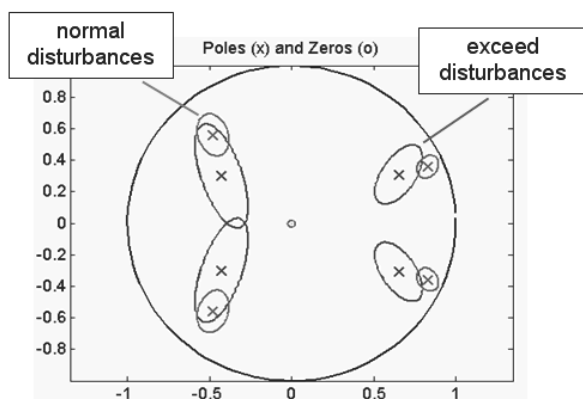

Fig. 2. Poles and zeros with confidence boundaries (ellipses) on the complex Z-plain in the case of normal and exceed disturbances

It is important to position the proposed method among other ones and discuss alternatives while considering its strengths and weaknesses. A brief survey on damage detection and location methods is presented in [13] outlining six categories, while discussion of typical machinery malfunctions is provided by [5,14]. Parametric methods are frequently used in modal analysis [15]. Early attempts of parametric modeling and modal analysis in rotor dynamics are given in [16], including rotor-bearing system identification from operational and experimental data, identification of a hydrodynamic bearing using a first-principle linearized model with adjustable parameters corresponding to stiffness and damping of the oil film, and advanced studies on the stability of hydrodynamic bearings. In the proposed approach, a faulty condition is detectable if pole coordinates cross the coordinates of 2D regions belonging to a given class, or a distance metric exceeds the value assigning a pole to a given class. A fault isolation is performed if the coordinates or membership metrics are known for each distinguishing class. Maintenance data and available plant specialist expertise are required to adjust the scenarios of pole placement in the case of malfunction occurrence and to transfer them into diagnostic patterns. This stage requires subjective judgments, because for non-typical machinery the patterns can be a priori unknown. However, this is also the case if

one uses currently available monitoring equipment. The alarm thresholds are adjusted based on the available domain knowledge, gathered measurement data, or simulation results [17]. Nevertheless, creation of scenarios in the proposed method can be supported by self-classification algorithms which preprocess the historical operational data (if available) by partitioning the search space and distributing the patterns in the resulting groups according to the values of their components. The uncertainty of pole location can be quantified using a statistical approach based on the standard deviation ellipses obtained for each pole. The inference (fault isolation) algorithm may use uncertainty estimates to involve confidence intervals assigned to particular classes. The problem of finding which, among a set of stored patterns, are closest to a given test pattern is of great general interest. There are effective real time applicable methods for coding of the diagnostic scenarios and knowledge [18,11], e.g. the nearest neighbor (NN) searching algorithm, fault or test trees, transition matrices, decision tables, diagnostic graphs, belief networks, and real time expert systems

The damping ratio and natural frequency are extracted from a particular eigenfrequency value to provide a direct physical meaning. Fig. 3 visualizes the concept where two classes of poles correspond to reference (healthy) and faulty operating conditions. In reality, the change of class can evolve (pending malfunction) and is preceded by a small deviation in pole locations. The sensitivity of the method depends on the measurement noise affecting model parameter estimation and modeling structure selection (model truncation).
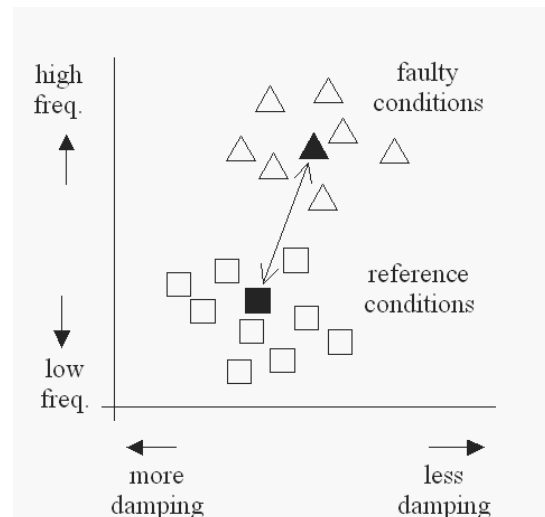

Fig. 3. Average pole placement as an estimate of rotating machinery conditions

Summing up, the method considers three stages: (i) parametric model identification based on the available transient data, (ii) extraction of model parameters (eigenfrequencies) in the form of poles located on a complex plain, and (iii) fault recognition based on the pattern of poles. The classification stage is performed on a priori partitioning regions belonging to normal and malfunctioned operational conditions.

3. Data-driven approach

The conducted experiments allowed the basic diagnostic relations to be identified based on pole placement. The rotor/bearing system [19] (Fig. 4) consists of a speed controller, 75 [W] electric motor, speed controller transducer, elastic coupling, phase-maker transducer (once per turn), laterally rigid with pivoting brass oilite bearing, 9.5 [mm] diameter steel shaft, four proximity eddy current transducers mounted in an XY orthogonal configuration respectively, a rotor disk of mass 0.8 kg with some unbalance, a four-radial spring supporting system, oil (T-10) lubricated bearing of 51 [mm] length, 220 [μm] radial clearance, and a four-port oil supply with up to 10.3 [kPa] pressure.

[ch#1 (horizontal), ch#2 (vertical)]

1. Oil Pump Assembly
2. Oil Bearing Assembly
3. Rotor Kit Shaft with Oil Bearing Journal
4. Preload Frame RK4 Rotor Kit Base with SFCB Option
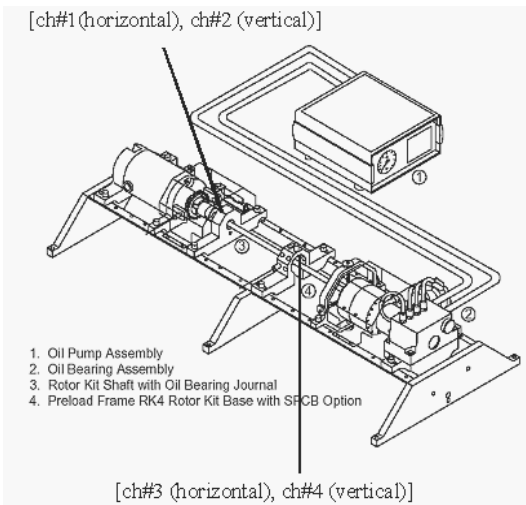
[ch#3 (horizontal), ch#4 (vertical)]

Fig. 4. R4 ROTOR KIT with oil pump assembly [19]

3.1. Test setup A and B

The objective of the presented test is the detection of changes in the dynamic response of a rotor-bearing system under normal and faulty operating conditions. The rotor was supported in the first configuration with two bronze bearings (Setup A, see Tables 1-2) and in the second configuration with a single bronze and a hydrodynamic bearing (Setup B, see Tables 1-2). Oil temperature was controlled to maintain oil viscosity at a constant level, in order to avoid oil file stiffness variation.

Eddy-current displacement transducers were mounted at the right bearing in the horizontal and vertical directions. Tests were performed with a rotor equipped with a single disk. A rotor during the test with Setups A and B was accelerated up to 7000 rpm in 140 sec to simulate transient operating conditions, and with the constant speed of 3000 rpm to simulate steady state operating conditions. The second-order AR(2) model was applied in the case of transient data (Setup A, B). AR model parameters were identified and transformed into the pole representation. The second order model has been selected. The confidence interval for a single pole is assumed as a triple

standard deviation [12]. System identification was performed several times separately for each collected data file to evaluate the scatter of pole placement. The beginning of the measured data is omitted, as marked in Table 1, e.g. waveforms starting at 10 sec. It allows the effects of initial rotor contact with stationary support components to be reduced. This contact may dramatically increase the bearing stiffness and disturb the system identification results.

Table 1.
Test rig configuration and signal length

Setup	Left support	Right support	Operating conditions	Analyzing signal part [s]	Total length of acquired signals [s]
A	Bronze bearing	Bronze bearing	Start up	10-90	0-140
B	Bronze bearing	Hydrodynamic bearing	Start up	10-90	0-140

Table 2.
System identification conditions

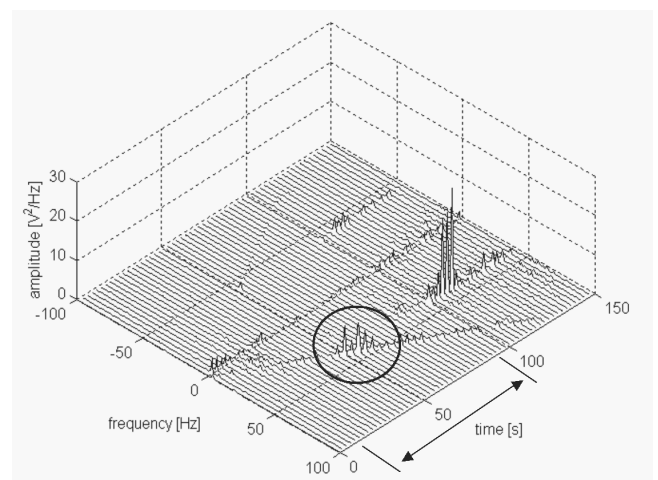| Setup	Model input	Model output	Applied model	Sampling frequency
A	Phase marker	Horizontal/vertical right bearing displacement signal	AR(2)	512
B	Phase marker	Horizontal/vertical right bearing displacement signal	AR(2)	512

Fig. 5. Spectrum waterfall plot of a complex signal of a journal position inside the hydrodynamic bearing under reference conditions (startup)

A few operating conditions were tested. The supply pressure inside the 360-degree hydrodynamic bearing was increased from

7 kPa up to 21 kPa using the external pump. The effect of a bearing instability can be easily achieved due to a high bearing clearance of 220 mm. The instability of a hydrodynamic bearing may lead to an increase in vibrations and further to the contact of a journal with the bearing surface. The looseness conditions were provided by the loose of 100mm at the hydrodynamic assembly screw. A preload of 10N was applied with a frame consisting of four springs and a centrally mounted friction bearing [19]. The unbalanced conditions were initialized by a mass of 2 mg attached (screwed) to the disk at selected angles.

The "black-box" model identification was performed on a selected part of the measured shaft displacement signals to exclude the data representing the unstable behavior of a rotor-bearing system above the 100-th sec (Fig. 5).

The selected signals consist of 10-90 sec. of the originally measured signals. This range covers the interaction of the first rotating speed component (1X) and the first bending natural frequency of a rotor resulted in a resonance at 50-th sec of startup.

3.2. Test results with setup A (looseness conditions)

The test rig has been configured to simulate loose assembly malfunctioning operation. A malfunction referring to bushing looseness may be caused in practice by a loose setscrew located on the top of the inboard bearing carrier (Fig. 6).
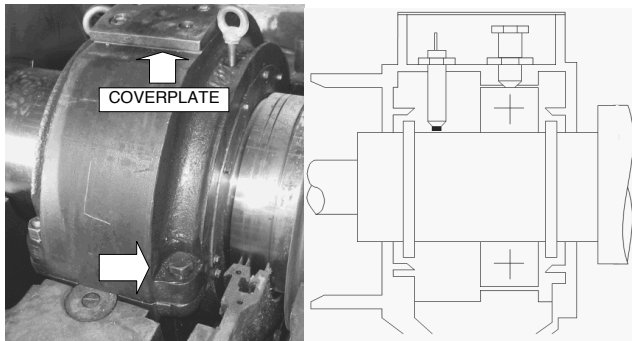

Fig. 6. The schematic shows the location of the setscrew (marked by an arrow) in the bearing housing
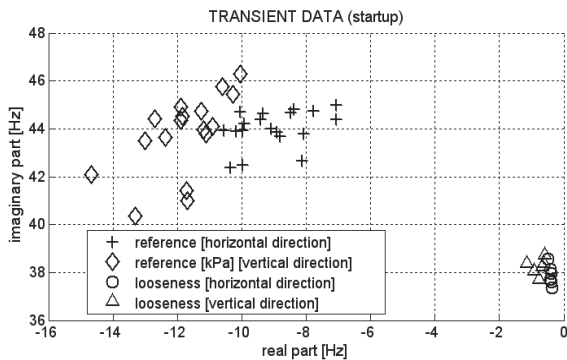

Fig. 7. Pole placement in reference and looseness conditions

In the investigated case, the looseness condition causes a significant drop in average natural frequencies; from 44 to 37.8 and from 42.7 to 38.2Hz for the horizontal and vertical directions, respectively. The average decay ratio also decreased dramatically (Figs. 7-8). This severe malfunction can be easily detected and isolated based on the pole placement.
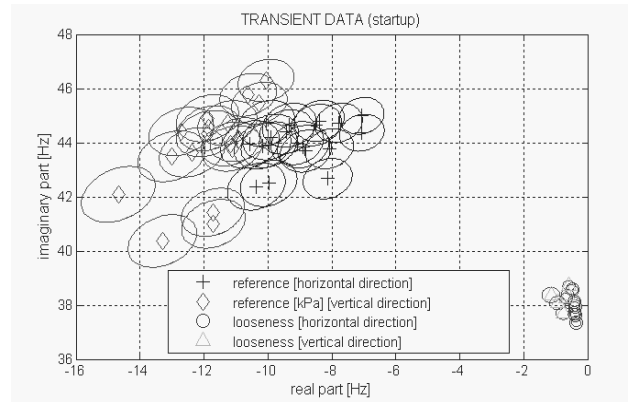

Fig. 8. Pole placement in reference and looseness conditions with confidence ellipses

The confidence ellipses were plotted for three standard confidence regions to show the uncertainty of pole placement (Fig. 8).

3.3. Test results with setup B (preload conditions)

The preload conditions were forced with the use of a frame equipped with a ball bearing and four springs controlling the preload force level in the horizontal and vertical directions [19].
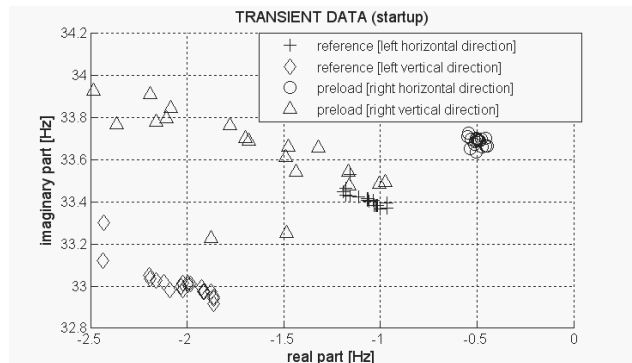

Fig. 9. Pole placement in reference and looseness conditions with confidence ellipses

The frame was mounted halfway between the disk and the hydrodynamic bearing. The spring system was set to a force of 10N preload in the vertical direction. The preload caused a theoretically expected [5] increase in rotor-bearing system

stiffness (Fig. 9). The average eigenfrequency value on a complex plain is substantially higher (by 0.5Hz) in the vertical direction where the preload was applied. The decay ratio dropped by 0.5 Hz in both directions.

4. First-principle approach

This section presents the physical rotor-support providing elementary quantification of rotating machine failure modes. The model involves numerous simplifications concerning a rotor and system of hydrodynamic bearings compared to a model formulated using finite element (FE) approach [6].

The model objective is to produce scenarios corresponding to experimental measurements in qualitative manner, and on the other hand create simulated data not affected by noise and systematic errors [13], e.g. a drift in eigenvalues caused by variable oil temperature.

4.1. Rotor model

A multi-support rotor model presented widely in literature [5-6,11] can be described using a matrix differential equation, where the subscripts n denote particular inertia, gyroscopic, damping, and stiffness forces associated with the n-th node:

$$\mathbf{M}\ddot{\mathbf{w}} + \mathbf{G}\dot{\mathbf{w}} + \mathbf{K}\mathbf{w} + f(\dot{\mathbf{w}}, \mathbf{w}) = \mathbf{u} \tag{1}$$

where:

$$\mathbf{w} = \begin{bmatrix} z \\ \varphi \end{bmatrix}, \ \mathbf{u} = \begin{bmatrix} u_z \\ u_\varphi \end{bmatrix}, \tag{2}$$

and, it yields to the following matrix equation:

$$\mathbf{M}_{n,n}\begin{bmatrix} \ddot{z}_n \\ \ddot{\varphi}_n \end{bmatrix} + \mathbf{G}_{n,n}\begin{bmatrix} \dot{z}_n \\ \dot{\varphi}_n \end{bmatrix} + \mathbf{K}_{n,n-1}\begin{bmatrix} z_{n-1} \\ \varphi_{n-1} \end{bmatrix} + \ldots$$

$$+ \mathbf{K}_{n,n}\begin{bmatrix} z_n \\ \varphi_n \end{bmatrix} + \mathbf{K}_{n+1}\begin{bmatrix} z_{n+1} \\ \varphi_{n+1} \end{bmatrix} + f(z_n, \dot{z}_n\varphi_n, \dot{\varphi}_n) = \begin{bmatrix} u_z \\ u_\varphi \end{bmatrix} \tag{3}$$

where $z_n = x_n + jy_n$, $\varphi_n = \theta_n + j\phi_n$. The expanded complex coordinates provide the matrix equation:

$$\mathbf{M}_{n,n}\begin{bmatrix} \ddot{x}_n \\ \ddot{y}_n \\ \ddot{\theta}_n \\ \ddot{\phi}_n \end{bmatrix} + \mathbf{G}_{n,n}\begin{bmatrix} \dot{x}_n \\ \dot{y}_n \\ \dot{\theta}_n \\ \dot{\phi}_n \end{bmatrix} + \mathbf{K}_{n,n-1}\begin{bmatrix} x_{n-1} \\ y_{n-1} \\ \theta_{n-1} \\ \phi_{n-1} \end{bmatrix} + \ldots$$

$$+ \mathbf{K}_{n,n}\begin{bmatrix} x_n \\ y_n \\ \theta_n \\ \phi_n \end{bmatrix} + \mathbf{K}_{n,n+1}\begin{bmatrix} x_{n+1} \\ y_{n+1} \\ \theta_{n+1} \\ \phi_{n+1} \end{bmatrix} + f(z_n, \dot{z}_n) = \ldots \tag{4}$$

$$= \Omega^2 \begin{bmatrix} m_n e_n \cos(\Omega t + \alpha_n) \\ m_n e_n \sin(\Omega t + \alpha_n) \\ -(I_{pn} - I_{Tn})\gamma_n \cos(\Omega t + \beta_n) \\ -(I_{pn} - I_{Tn})\gamma_n \sin(\Omega t + \beta_n) \end{bmatrix}$$

The above equation considers the coupled rotor motion in the translational and rotational coordinates as described in [5-6]. The equations can be expanded of nonlinear terms modeling influence of disturbances which affect eigenvalues through nonlinear relations, as follows:

$$\mathbf{M}\ddot{\mathbf{w}} + \mathbf{G}\dot{\mathbf{w}} + \mathbf{K}\mathbf{w} + f(\dot{\mathbf{w}}, \mathbf{w}) + g(\dot{\mathbf{w}}, \mathbf{w}) = \mathbf{u} \tag{5}$$

4.2. Rotor support models

A rotor is always support with bearings which are essential parts of the rotating machinery influencing its dynamics and frequency response. The support model available in the model discussing in this paper were described in this sub-section.

There are two main groups of hydrodynamic bearing designs: circular and non circular with fixed and tilting pads. Nowadays, elliptical, multiple-lobe, and tilting pad non circular bearing, are commonly use in industrial applications since they offer the most stable machinery operation. These types of bearings are extension of conventional circular bearings which are considered in this section. A circular bearing consist of two cylinders of different radii, characterized the radial clearance c, and ratio of length to external cylinder diameter L/D. The most simplified bearing model is a heuristic model [5] which is adequate for lightly loading seals and bearings. This model considers a quasi-concentric solid body rotating inside or outside a stationary body assuming the following: (i) the rotating component is appropriately aligned, (ii) full fluid flow is kept at a constant level all the time, (iii) the fluid flows at a rate of $\lambda\Omega$, (iv) any axial motion of fluid is independent of the circumferential motion, (v) the stiffness of the fluid film increases along the size of eccentricity. The forces F_x and F_y generated by the fluid film are obtained with the following equation of a nonlinear heuristic model [5]:

$$f(z_n, \dot{z}_n) = \begin{bmatrix} F_x \\ F_y \end{bmatrix} = \begin{bmatrix} m_r & 0 \\ 0 & m_r \end{bmatrix}\begin{bmatrix} \ddot{x} \\ \ddot{y} \end{bmatrix} + \ldots$$

$$+ \begin{bmatrix} d & 2\lambda\Omega m_r \\ -2\lambda\Omega m_r & d \end{bmatrix}\begin{bmatrix} \dot{x} \\ \dot{y} \end{bmatrix} + \ldots$$

$$+ \begin{bmatrix} k_0 - \lambda^2\Omega^2 m_r & \lambda\Omega d \\ -\lambda\Omega d & k_0 - \lambda^2\Omega^2 m_r \end{bmatrix}\begin{bmatrix} x \\ y \end{bmatrix} + \ldots \tag{6}$$

$$+ \begin{bmatrix} \Psi_2(|e|) & 0 \\ 0 & \Psi_2(|e|) \end{bmatrix}\begin{bmatrix} \dot{x} \\ \dot{y} \end{bmatrix} + \ldots$$

$$+ \begin{bmatrix} \Psi_1(|e|) & \lambda\Omega\Psi_2(|e|) \\ -\lambda\Omega\Psi_2(|e|) & \Psi_1(|e|) \end{bmatrix}\begin{bmatrix} x \\ y \end{bmatrix}$$

where ψ_1 and ψ_2 are nonlinear stiffness and damping functions of the rotor radial displacement:

$$\Psi(e) = \kappa\left(1 - \frac{e^2}{c^2}\right)^{-3} \tag{7}$$

The physical bearing model is based on the Reynold's equation and allows to analyze the oil flow in a determined layer, comprising the balance equations for a fluid element and the equations of flow continuity. Reynold's equation [22] provides better insight in the dynamics of a rotor-bearing system especially under transient conditions when a nonlinear dynamic analysis needs to be carried out. The equation does not posses analytical solution, except simplified cases such as proposed by Sommerfeld infinitely long bearing model neglecting the axial flow and proposed by Ocvirk short bearing model. The solutions can differ taking into account boundary conditions assumed by Sommerfeld, Gümbel, or Reynold. The basic Reynold's equation has the form:

$$\frac{\partial}{\partial x}\left(\frac{h^3}{12\mu}\frac{\partial p}{\partial x}\right)+\frac{\partial}{\partial z}\left(\frac{h^3}{12\mu}\frac{\partial p}{\partial z}\right)=\frac{1}{2}R\cdot\Omega\frac{\partial h}{\partial x}+\frac{\partial h}{\partial t} \qquad (8)$$

involving the following assumptions: (i) lubricating oil is Newtonian fluid, (ii) constant viscosity and density are specific to lubricating oil (isothermal process), (iii) laminar flow occurs, (iv) mass forces of lubricating oil particles are negligible, (v) shaft motion has a stable characteristic, and the shaft center is held in its position, (vi) the shaft and the bearing bushing are not deformed; they ideally smooth/even and shaped in the form of cylinders, (vii) pressure prevailing in the lubricating oil layer remains unchanged along the layer thickness. The Reynolds equation written in the coordinate system x=Rq, and z is as follows:

$$\frac{1}{R^2}\frac{\partial}{\partial\theta}\left(\frac{h^3}{12\mu}\frac{\partial p}{\partial\theta}\right)+\frac{\partial}{\partial z}\left(\frac{h^3}{12\mu}\frac{\partial p}{\partial z}\right)=\frac{1}{2}\Omega\frac{\partial h}{\partial\theta}+\frac{\partial h}{\partial t} \qquad (9)$$

The two assumptions that can be made are an infinitely short and long (or perfectly sealed) bearing. The short bearings are used more often because there is a possibility that small shaft deflections or misalignment can reduce the radial clearance to zero in long bearings. For short bearing the end leakage can be a significant factor. The forces F_x and F_y generated by the fluid film are obtained based on the analytical solution of Reynold's equation for short bearing approximation [22]:

$$f(z_n,\dot{z}_n)=$$
$$\left[\begin{array}{l}F_x=-\mu\pi R L^3\left[\dfrac{\Omega y_n+2\dot{x}_n}{2(c^2-x_n^2-y_n^2)^{3/2}}+\dfrac{3x_n(x_n\dot{x}_n+y_n\dot{y}_n)}{2(c^2-x_n^2-y_n^2)^{5/2}}\right]\\[4mm]F_y=-\mu\pi R L^3\left[\dfrac{2\dot{y}_n-\Omega x_n}{2(c^2-x_n^2-y_n^2)^{3/2}}+\dfrac{3y_n(x_n\dot{x}_n+y_n\dot{y}_n)}{2(c^2-x_n^2-y_n^2)^{5/2}}\right]\end{array}\right] \qquad (10)$$

in case of infinitely long bearings the axial flow is neglected assuming no end leakage of oil from the bearing. This assumption is acceptable for a bearing with L/D > 4 and negative pressure regions may occur depending on supply pressure [22]. The Reynold's equation for the infinitely long bearing approximation is derived as follows [21]:

$$\frac{1}{R^2}\frac{\partial}{\partial\theta}\left(\frac{h^3}{\mu}\frac{\partial p}{\partial\theta}\right)=6\Omega\frac{\partial h}{\partial\theta}+12\frac{\partial h}{\partial t} \qquad (11)$$

and finally after substitution:

$$\frac{1}{R^2}\frac{\partial}{\partial\theta}\left[\frac{h^3}{\mu}\frac{\partial p}{\partial\theta}\right]=6\left[(\Omega-2\dot{\alpha})\frac{\partial h}{\partial\theta}+2\dot{\beta}\cos(\theta)\right] \qquad (12)$$

The forces F_x and F_y generate by the fluid film can be obtained via Reynold's equation regarding assumptions [21]:

$$F_\beta=-\frac{12\mu R^3 L}{c^2}\left[\frac{\beta_n^2(\Omega-2\dot{\alpha})}{(1-\beta_n^2)(2+\beta_n^2)}+\frac{\beta_n\cdot\dot{\beta}_n}{(1-\beta_n^2)}+\ldots\right.$$
$$\left.+\frac{2\dot{\beta}_n}{\sqrt{(1-\beta_n^2)^3}}\arctan\sqrt{\frac{1+\beta_n}{1-\beta_n}}\right]$$
$$F_\alpha=\frac{6\pi\mu R^3 L}{c^2}\frac{\beta_n(\Omega-2\dot{\alpha}_n)}{\sqrt{(1-\beta_n^2)(2+\beta_n^2)}} \qquad (13)$$

The total force component in the x and y can be obtained in the following way [21]:

$$f(z_n,\dot{z}_n,)=\left[\begin{array}{l}F_\beta\cos\theta-F_\alpha\sin\theta\\F_\beta\sin\theta+F_\alpha\cos\theta\end{array}\right];$$
$$x_n=c\cdot\beta_n\cdot\cos(\alpha_n);$$
$$y_n=c\cdot\beta_n\cdot\sin(\alpha_n)$$
$$\beta_n=\frac{\sqrt{x_n^2+y_n^2}}{c},\alpha_n=\arctan\left(\frac{y_n}{x_n}\right) \qquad (14)$$

Heuristic, infinitely short and long bearing models have been implemented in Simulink model together with a rotor model, and parameterized according to the rotor test rig geometry, physical properties, and configuration [21].

4.3. Model application and malfunctions modeling

This test rig consists of a flexible rotor supported with a single sliding/hydrodynamic bearing characterized with physical and geometrical parameters presented in Tables 3-6. The rotor model consists of 17 nodes and 16 rotor sections (Fig. 10). The model can simulate startup/cost down and steady state operating conditions.
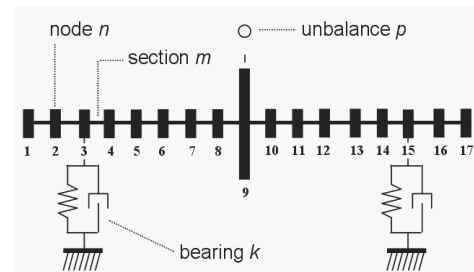
Fig. 10. Rotor model discrete representation

Table 3.
Model properties linked with nodes

		Node 1	Node 2
Unbalance	radius [m]	0.035	0
	mass [gram]	2	0
	phase [°]	0	0
Physical parameters	mass of disk	1.9	0.2
Bearings (short hydrodynamic bearing approximation)	clearance [μm]	-	200
	viscosity [Pa·s]	-	0.01
	length L [m]	-	0.0225
	diameter D [m]	-	0.055

Table 4.
Model properties linked with shaft sections

		section 1
Rotor properties	length of section [m]	0.22
	shaft diameter [mm]	5

Table 5.
Rotor properties corresponding to nodes

		rotor section #		
		1-2	3-14	15-16
Rotor properties	length of section [mm]	25	40	20
	shaft diameter [mm]	9.5	9.5	9.5

Table 6.
Shaft properties corresponding to rotor sections

		rotor node #						
		1-2	3	4-8	9	10-14	15	16-17
Unbalance	radius [m]	0	0	0	0.035	0	0	0
	mass [g]	0	0	0	0.2	0	0	0
	phase [°]	0	0	0	0	0	0	0
Disc	mass of disk [kg]	-	-	-	0.8	-	-	-
Support models — Physical	clearance [μm]	-	-	-	-	-	220	-
	viscosity [Pa·s]	-	-	-	-	-	0.02	-
	length L [m]	-	-	-	-	-	0.03	-
	diameter D [m]	-	-	-	-	-	0.051	-
	elevation [m]	-	-	-	-	-	0	-
Support models — heuristic	average fluid velocity [-]	-	-	-	-	-	0.48	-
	fluid damping [Ns/m]	-	-	-	-	-	3700	-
	fluid mass [kg]	-	-	-	-	-	0.1	-
Support models — Sliding bearing	vertical stiffness [N/m]	-	0.24 E6	-	-	-	-	-
	Horizontal stiffness [N/m]	-	0.24 E6	-	-	-	-	-
	vertical damping [Ns/m]	-	1E5	-	-	-	-	-
	Horizontal damping [Ns/m]	-	1E5	-	-	-	-	-

The presented model provides rank correlation (Fig. 11) with observed phenomena and allows to quantify eignevalues sensitivity to particular malfunctions [9]. For that purpose, this model is extended of functionality enabling modeling of fundamental malfunctions, e.g. anisotropic rotor properties, full angular or rotor-to-stationary part rubbing contact, or looseness.
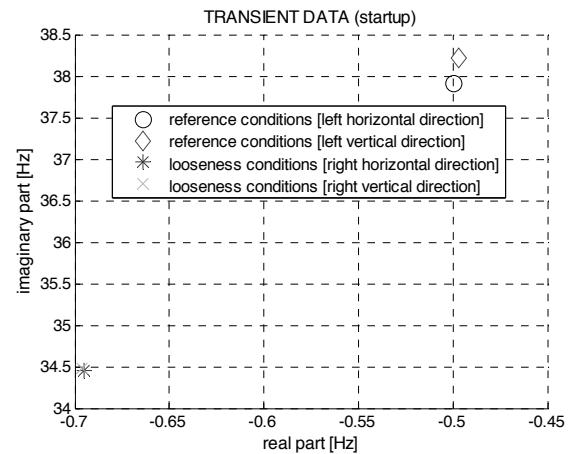

Fig. 11. Pole placement in reference and looseness conditions with confidence ellipses

The eignevalues of a nonlinear system depends on a type of excitation being also a source of numerous malfunctions, e.g. a rotor unbalance. A mechanical rotor-bearing systems is very sensitive to the periodic excitation frequency considering discontinuous and/or piece-wise nonlinearities activated by motion of the system elements. This type of systems response consists of original periods and certain multiple periods of the exciting force. A mechanical structure with looseness at either a stationary or rotating joint, and the rotor, which occasionally rubs with the stator, belong to this class of systems [9]. The stiffness in these systems vary between extreme discrete values; higher stiffness results when there is contact at the joint (or rubbing location), and lower stiffness occurs when the substructures separate [5]. Similarly, damping characteristics of the system may alternate. Additional friction-related effects occur at the substructure contact locations, when their relative motion takes place [5].

5. Hardware implementation

The hardware realization of the proposed method is considered as a standalone operating module enabling fault detection (Figs. 12-13) [23-24]. A prototype vibration analyzer module was developed based on the Texas Instruments TMS3200LF2407 Starter Kit. A library of non-parametric and parametric system identification algorithms has been developed as C-codes routines. This library provides access to conventional Fourier-based and AR/ARX parametric models that are adaptable for various target platforms, e.g. microcontrollers, DSP, and PC-based applications in SCADA systems. A Texas Instrument

C-Compiler generates an assembler-code, which is downloaded via an RS232 interface to the DSP. The link for the Code Composer Studio® Development Toolbox available in Matlab can be used to accelerate code controlling and debugging through a direct link between Matlab and the development board. The hardware implementation solution has been first tested based on the software emulator in the Matlab environment.
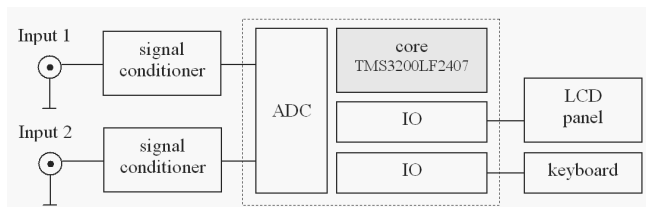

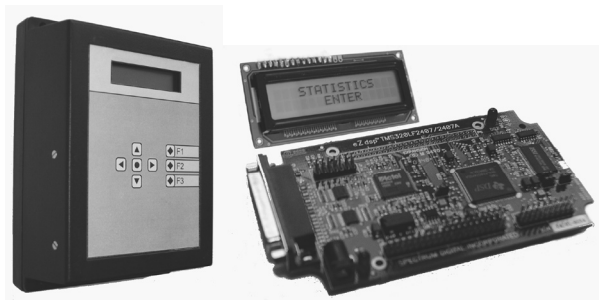Fig. 12. Hardware architecture of the prototype vibration machinery analyzer

Fig. 13. Prototype Vibration Machinery Analyzer consists of input hardware filters, internal DSP module, and display

6. Summary

The high performance of rotating machinery is one of the key factors in the proper management of plant assets. Therefore, the paper deals with the development of techniques designed for the experimental vibration analysis of rotating machinery from the viewpoint of system analysis. Such an experimental vibration analysis has been used to describe the dynamic behavior of a rotor supported by sliding or hydrodynamic bearings in terms of natural frequencies, as well as damping factors. The paper presents research and development concerning model-based rotor diagnostics with the use of a parametric model.

Acknowledgements

Nomenclature

Ω - rotating speed [1/s],

L - total rotor length [m],

a - distance between beginning of a rotor and the considering node [m],

b - distance between end of a rotor and the considering node [m],

x, y - lateral motion coordinates [m],

z - coordinate along the shaft axis [m],

$\theta = dx/dz$ - coordinate in angular motion [rad],

$\phi = dy/dz$ - coordinate in angular motion [rad],

n - the index of the node [-],

N - the total number of nodes multiply by 4 degree of freedom (corresponding to two for vertical and two for translational vibrations) for all local matrices assosiated with the nodes,

w - global response vector of translational and rotational vibrations of size Nx1,

u - global excitation vector of translational and rotational vibrations of size Nx1,

M - global inertia matrix of translational and rotational vibration of size NxN,

G - global gyroscopic matrix of translational and rotational vibrations of size NxN,

K - global stiffness matrix of translational and rotational vibrations of size NxN,

$\mathbf{w}_n$ - local response vector of translational and rotational vibrations for the n-th node,

$\mathbf{u}_n$ - local excitation vector of translational and rotational vibrations for the n-th node,

$\mathbf{M}_n$ - local inertia matrix of translational and rotational vibration for the n-th node,

$\mathbf{G}_n$ - local gyroscopic matrix of translational and rotational vibrations for the n-th node,

$\mathbf{K}_n$ - local stiffness matrix of translational and rotational vibrations for the n-th node,

m_r - fluid mass [kg],

λ - average fluid velocity [-],

d - damping coefficient of a fluid film [N·s/m],

k_0 - stiffness coefficients of a fluid film [N/m],

ε - relative eccentricity of journal [-],

e - bearing eccentricity determining a distance of the center of the journal from the center of the bearing bushing [m],

c - bearing clearance [m],

μ - dynamic viscosity [Pa·s],

θ - current angular position of the journal centre [rad],

h - dimensional oil gap (oil film thickness) [m],

L - length of the journal [m],

R - journal radius [m],

p - oil pressure [Pa],

f(.) - nonlinear function [N],

m - mass [kg],

I_T - transverse inertia moment [kg·m^2],

I_P - polar inertia moment [kg·m^2],

I - area moment [m^4],

l - length of shaft section [m],

d - diameter of shaft section [m],

κ - initial bearing stiffness/damping [N/m]/[Ns/m],

ρ - density [kg/m^3],

E - Young's modulus [N/m^2],
l - length of the shaft [m],
μ - Poisson constant [-].

References

[1] T. Dzitkowski, A. Dymarek, Design and examining sensitivity of machine driving systems with required frequency spectrum. Journal of Achievements in Materials and Manufacturing Engineering 26/1 (2008) 49-56.

[2] A. Buchacz, S. Żółkiewski, Dynamic analysis of the mechanical systems vibrating transversally in transportation, Journal of Achievements in Materials and Manufacturing Engineering 20 (2007) 331-334.

[3] S. Żółkiewski, Analysis and modelling of rotational systems with the modify application, Journal of Achievements in Materials and Manufacturing Engineering 30/1 (2008) 59-66.

[4] K. Białas, Synthesis of mechanical systems including passive or active elements reducing of vibrations, Journal of Achievements in Materials and Manufacturing Engineering 20 (2007) 323-326

[5] A. Muszynska, Rotordynamics, Taylor & Francis Group, LLC, Minden, USA, 2005.

[6] E Krämer, Dynamics of Rotors and Foundations, Springer-Verlag, Berlin, 1993.

[7] V. Wowk, Machinery Vibration. Measurement and Analysis, McGraw-Hill, US, 1991.

[8] R.C. Eisenmann, Machinery Malfunction Diagnosis and Correction, Hewlett Packard Professional Books, New Jersey, 1997.

[9] Allianz, Allianz Handbook of Loss Prevention, Allianz Versicherung AG, Berlin and Munich, Germany, 1987.

[10] Bently Nevada, Vibration Analysis for Power Plant. Intercompany materials, Mindem, US, 19994.

[11] R.J. Patton, P.M. Frank, R N Clark (eds.), Issues of fault diagnosis for dynamic systems, Springer-Verlag, London, 2000.

[12] L. Ljung, System Identification - Theory for the User, Prentice-Hall, 1999.

[13] M.I. Friswell, J.E.T. Penny, The Practical Limits of Damage Detection and Location using Vibration Data, Proceedings of the 11th VPI&SU Symposium on Structural Dynamics and Control, Blacksburg, Virginia, US, 1997.

[14] M.L. Adams, Rotating Machinery Vibrations. Form Analysis to Troubleshooting, Marcel Dekker, New York, 2001.

[15] M.I. Friswell, J.E.T. Penny, S.D. Garvey, Parameter Subset Selection in Damage Location, Inverse Problems in Engineering 5/3 (1997) 189-215.

[16] O Mahrenholtz (ed.), Dynamics of Rotors. Stability and System Identification, Springer-Verlag, Wien - New York, 1984.

[17] Bently Nevada, Specifications and Ordering Information. Machine Condition Manager 2000, (http://www.bently.com).

[18] W. Cholewa, Real time diagnostic expert systems for steam turbines, KARNTEKNIK 2000, Stockholm, 2000, 221-222.

[19] Bently Nevada, 'Rotor Kit and Oil Whirl/Whip Option', Bently Nevada Corporation, Minden, US, 1994.

[20] MATLAB, The Math Works Inc., Natick, 1998.

[21] P.M. Przybylowicz, Active stabilization of a rigid rotor by a piezoelectrically controlled mobile journal bearing system, Sixth International Conference on Rotor Dynamics Proceedings, Sydney, Australia, 2002, 79-84.

[22] J. Frene, D. Nicolas, B. Deguerce, D. Berthe, M. Godet, Hydrodynamic Lubrication, Bearings and Thrust Bearings, Elsevier Science B.V., Amsterdam, 1997.

[23] J. Świder, A. Baier, Designing assist of virtual building and researching modern control systems, Journal of Achievements in Materials and Manufacturing Engineering 11 (2002) 537-540 (in Polish).

[24] J. Świder, R. Zdanowicz, Application of PLC controller in models systems simulation, Journal of Achievements in Materials and Manufacturing Engineering 12 (2003) 561-564 (in Polish).